Lipopolysaccharide-induced down-regulation of Ca^{2+} release-activated Ca^{2+} currents (I_{CRAC}) but not Ca^{2+}-activated TRPM4-like currents (I_{CAN}) in cultured mouse microglial cells

Andreas Beck, Reinhold Penner and Andrea Fleig

Queen's Center for Biomedical Research, Laboratory of Cell and Molecular Signalling, The Queen's Medical Center and John A. Burns School of Medicine, University of Hawaii, Honolulu, HI 96813, USA

Microglia are the main immunocompetent cells of the mammalian central nervous system (CNS). Activation of cultured microglial cells and subsequent release of nitric oxide and cytokines critically depends on intracellular calcium levels. Since microglia undergo dramatic morphological, biochemical and electrophysiological changes in response to pathological events in the CNS, we investigated temporal changes in expression levels of ion channels involved in cellular calcium homeostasis in mouse cortical microglial cells in culture. Specifically, we assessed the inward and delayed outward rectifier potassium currents (I_{IRK} and I_{DRK}), calcium (Ca^{2+}) release-activated Ca^{2+} currents (I_{CRAC}) and Ca^{2+}-activated TRPM4-like currents (I_{CAN}) in non-activated microglia and cells that were activated by exposure to lipopolysaccharide (LPS) between 3 and 48 h. Unstimulated microglial cells, subcultured from an astrocyte coculture, typically exhibited a ramified, rod-shaped morphology. During the first 3 days of culture cell size and shape were maintained, but the percentage of cells showing prominent I_{IRK} went up and those expressing I_{DRK} went down. Cells retaining I_{DRK} exhibited smaller amplitudes, whereas those of I_{IRK} and I_{CRAC} were not affected. However, after 24 h of exposure to 1 μg ml^{-1} LPS, most cells showed an amoeboid ('fried egg'-shaped) morphology with a 62% increase in cell capacitance. At that point in time, only 14% of the cells revealed I_{IRK} and 3% had I_{DRK} exclusively, whereas the majority of cells expressed both currents. The amplitudes of I_{CRAC} and I_{IRK} progressively decreased after stimulation, whereas I_{DRK} transiently reached a maximum after 6 h of LPS exposure and then returned to pre-stimulation expression levels. Cultured microglia also revealed TRPM4-like, Ca^{2+}-activated non-selective currents (I_{CAN}) with an EC_{50} of 1.2 μM $[Ca^{2+}]_i$. The expression levels of this current did not change significantly during and after 24 h of LPS exposure. We propose that LPS-induced down-regulation of I_{IRK} and I_{CRAC} will reduce the cell's capacity to produce significant calcium influx upon receptor activation and result in decreased sensitivity to exogenous stimulation. In this scenario, I_{CAN} expression would remain constant, although its activity would automatically be reduced due to the diminished calcium influx capacity of the cell.

(Received 17 September 2007; accepted 7 November 2007; first published online 8 November 2007)
Corresponding author A. Beck: Queen's Center for Biomedical Research, Laboratory of Cell and Molecular Signalling, The Queen's Medical Center and John A. Burns School of Medicine, University of Hawaii, Honolulu, HI 96813, USA. Email: abeck@queens.org

Microglia derive from cells of the monocytic lineage entering the brain from the bloodstream during early embryonic development. They differentiate into brain resident cells and become the main immune effector cells in the CNS. Microglia are recognized for their scavenging function in response to pathological events (McGeer *et al.* 1988; Dickson *et al.* 1991; Bo *et al.* 1994; McGeer & McGeer, 1995; Meda *et al.* 1995; Baker & Manuelidis, 2003; Streit *et al.* 2004; Jack *et al.* 2005; Sargsyan *et al.* 2005; Conde & Streit, 2006; Wang *et al.* 2007).

Microglia appear in three different shapes as ramified, amoeboid and intermediate cells (del Rio Hortega, 1932; Kershbaum, 1939) and three different physiological states as resting, activated and amoeboid-phagocytic cells (Streit *et al.* 1989; Sasaki *et al.* 1993). Ramified microglia, representing 5–20% of all glia in the normal

 DOI: 10.1113/jphysiol.2007.145151

CNS (Lawson *et al.* 1990), is often referred to as resting microglia, since they respond to insults such as infection, traumatic injury or ischaemia by converting into amoeboid macrophage-like cells that move towards the site of injury (Thomas, 1992; Vilhardt, 2005). Following activation, microglia change their shape and express a distinct pattern of ion channels linked to their activation state (Norenberg *et al.* 1994; Biro *et al.* 1998; Farber & Kettenmann, 2005). Cultured microglia mainly express voltage-independent inward and, depending on the state of activation, voltage-gated outward potassium currents (Norenberg *et al.* 1992, 1994; Pyo *et al.* 1997; Eder, 1998; Walz & Bekar, 2001). However, microglia of freshly isolated rat cortical brain slices reveal little, if any, inward potassium or voltage-gated membrane currents (Boucsein *et al.* 2000). Thus, cultured microglial cells might not represent the fully resting state of microglia *in vivo*, although they remain responsive to a variety of stimuli that induce further changes in microglial properties.

The by far most frequently used model stimulus to study microglia activation and inflammatory signalling is the Gram-negative bacterial cell-wall component lipopolysaccharide (LPS). LPS activates the microglial Toll-like receptor-4 (TLR-4) and induces the transcription of genes that are involved in initiation or regulation of the inflammatory response (Hoshino *et al.* 1999; Lee & Lee, 2002). As a result, microglial cells change their shape (abd-el Basset & Fedoroff, 1995; Kloss *et al.* 2001), express various secretory compounds such as cytokines/chemokines, growth factors, tumour necrosis factor-α (TNF-α), super-oxide, nitric-oxide (NO) and prostaglandin E_2 (PGE_2) (Nakamura *et al.* 1999; Ajmone-Cat *et al.* 2003; Rock *et al.* 2004), and show increased expression levels of glutamate transporter 1 (GLT-1) (Persson *et al.* 2005). They develop inward rectifying potassium currents (I_{IRK}) *in vivo* (cultured miroglia already show I_{IRK}, see above and present study) and voltage-gated, delayed rectifying potassium currents (I_{DRK}) carried by Kv1.3 and/or Kv1.5 channels in culture and Kv1.5 *in vivo* (Kettenmann *et al.* 1990; Norenberg *et al.* 1992, 1994; Pyo *et al.* 1997; Jou *et al.* 1998; Boucsein *et al.* 2000). LPS also induces calcium (Ca^{2+}) transients in cultured microglial cells, possibly resulting from caffeine-sensitive Ca^{2+} release (Bader *et al.* 1994) and/or dependent on Ca^{2+} influx (Herms *et al.* 1997; Choi *et al.* 2002; Yi *et al.* 2005). A permanent elevation of the basal Ca^{2+} concentration along with a suppression of UTP-evoked Ca^{2+} signalling has also been described for LPS-exposed cultured microglial cells (Hoffmann *et al.* 2003).

A recent model, first established in Jurkat T cells, proposes that several ion channels act in concert to shape calcium signals in immune cells (Launay *et al.* 2004). Here, TRPM4, a Ca^{2+}-activated non-selective (CAN) channel and Ca^{2+} release-activated Ca^{2+} currents (I_{CRAC}), as well as Kv1.3 and K_{Ca} control intracellular Ca^{2+} oscillations through oscillatory changes in membrane potential (Launay *et al.* 2004). Since LPS-induced chronic elevation of intracellular Ca^{2+} attenuates receptor-induced Ca^{2+} signals in activated microglia cells (Hoffmann *et al.* 2003), we wondered whether this would be achieved by an LPS-induced change not only in I_{IRK} or I_{DRK}, but also I_{CRAC} and CAN channels, if the latter were expressed in cultured microglial cells. Since most studies have only assessed endpoint states of microglia activation, we also wanted to learn about the kinetics of ion channel expression, particularly with respect to early effects (< 24 h) of LPS.

We therefore set out to first confirm the presence of Ca^{2+}-activated TRPM4-like currents in microglial cells. We then established a temporal profile of morphological and electrophysiological changes in cultured cortical mouse microglial cells over a period of 7 days in subculture and early responses to continuous exposure to 1 μg ml^{-1} LPS as a model of microglial cell activation. We used the patch-clamp technique to investigate LPS-dependent changes of inward and delayed outward rectifier potassium currents (I_{IRK} and I_{DRK}), Ca^{2+} release-activated Ca^{2+} currents (I_{CRAC}) and Ca^{2+}-activated TRPM4-like currents (I_{CAN}) in non-activated and LPS-stimulated cultured mouse microglial cells.

Methods

Preparation and culture of mouse microglial cells

Microglial cells were obtained from cortex of mouse pups (postnatal days 0–2) as previously described (Giulian & Baker, 1986). In brief, pups were decapitated in accordance with the University of Hawaii Institutional Animal Care and Use Committee guidelines after anaesthesia with enflurane (5–10 drops onto tissue in 200 ml beaker), and their brains were collected under sterile conditions in basal Eagle's medium (BME, Gibco). Cortices were dissected, the meninges removed, and triturated after enzymatic digestion with 0.25% trypsin/5.26 mM EGTA and washing in glial medium (BME supplemented with 1% L-glutamine and 2 ml l^{-1} penicillin–streptomycin). The homogenate was then forced through a 20 nm filter and the resulting suspension was plated in 75 cm^3 poly L-lysine-coated culture flasks containing glial medium with 10% fetal bovine serum (FBS). The cells were kept in an incubator at 37°C and 5% CO_2, and the medium was changed 3 days following preparation and once per week thereafter. After about 3–4 weeks in culture, the flasks showed a confluent layer of astrocytes with microglial cells growing on its surface. Microglial cells were harvested and isolated by shaking the flasks to release the loosely attached microglia into the supernatant. Microglia from the supernatant were washed and plated on poly L-lysine-coated glass coverslips in glial medium with 5% FBS. Plated cells were used for patch clamp experiments 1–7 days after harvest. To

allow the cells to adapt to the subculture conditions, LPS experiments started 3 days after harvest. For microglia activation, 1 μg ml^{-1} lipopolysaccharide (LPS) was added to the media 3–48 h before starting patch-clamp experiments.

Salines

All salines were freshly prepared from refrigerated stock solutions. The external saline to measure inward and delayed outward rectifying potassium currents (I_{IRK}, I_{DRK}) was composed of (mM): NaCl 140, KCl 10, $CaCl_2$ 1, $MgCl_2$ 2, glucose 10, Hepes-NaOH 10, pH 7.2. The external solution for TRPM4-like currents contained 2.8 mM KCl and for I_{CRAC} recordings, 2.8 mM KCl and 10 mM $CaCl_2$. Intracellular pipette-filling solutions for I_{IRK} and I_{DRK} contained (mM): potassium glutamate 140, NaCl 8, $MgCl_2$ 1, Hepes-KOH 10, pH 7.2; for I_{CRAC} (mM): caesium glutamate 140, NaCl 8, $MgCl_2$ 1, Cs-BAPTA 10, $InsP_3$ 0.02, Hepes-CsOH, pH 7.2. Pipette-filling solutions for TRPM4-like currents were the same as for I_{IRK} and I_{DRK}, but $[Ca^{2+}]_i$ was buffered to elevated levels by adding 10 mM K-BAPTA and an appropriate amount of $CaCl_2$ (calculated with WebMaxC http://www.stanford.edu/~cpatton/webmaxcS.htm). The osmolarity of all solutions ranged between 285 and 305 mosmol l^{-1}. All salts were obtained from Sigma.

Patch-clamp experiments

Coverslips with subcultured microglial cells were transferred to a recording chamber and kept in the modified Ringer solution described above. Patch pipettes were prepared from borosilicate glass capillaries (inner diameter 1.5 mm, Kimble products) using a horizontal puller (Sutter Instruments, Modell P-97), fire-polished, and had resistances between 2 and 4 MΩ. Patch-clamp experiments were performed in the tight-seal whole-cell configuration at room temperature (22–24°C). High-resolution current recordings were acquired by a computer-based patch-clamp amplifier system (EPC-9, HEKA). For I_{CRAC} recordings, voltage ramps of 50 ms duration spanning a voltage range of −130 to 100 mV over 50 ms were delivered from a holding potential (V_h) of 0 mV every 2 s over a period of 200 s. For I_{IRK} and I_{DRK} measurements, ramps from −130 to 100 mV were applied with $V_h = -60$ mV. Calcium-activated (TRPM4-like) currents were measured using ramps from −100 to 100 mV at a V_h of 0 mV and for 350 s. All voltages were corrected by a 10 mV liquid junction potential. Currents were filtered at 2.9 kHz and digitized at 100 μs intervals. Capacitive currents and series resistance were determined and corrected before each voltage ramp using the automatic capacitance compensation of the EPC-9. In I_{CRAC} experiments, the first one to three ramps were subtracted from all following ramps to subtract background conductances. The low-resolution temporal development of currents at a given potential was extracted from individual ramp current recordings by measuring the current amplitudes at voltages of −110 mV for I_{IRK} and I_{CRAC}, +80 mV for I_{DRK} and −80 mV and +80 mV for TRPM4-like currents. All currents were normalized to cell size to obtain current densities (pA pF^{-1}).

Fura-2 Ca^{2+} measurements

For Ca^{2+} measurements, cells were loaded with 1 μM Fura-2 AM (acetoxymethylester, Molecular Probes) for 60 min in media at 37°C, washed and kept in external solution containing (mM): NaCl 140, KCl 2.8, $CaCl_2$ 1, $MgCl_2$ 2, glucose 10, Hepes-NaOH 10, pH 7.2. The Ca^{2+}-dependent Fura-2 fluorescence of several cells was monitored at a rate of 0.2 Hz with a dual excitation fluorometric imaging system (TILL-Photonics, Gräfelfingen, Germany) controlled by TILLvisION software, using a Zeiss Axiovert 100 fluorescence microscope equipped with a 40× Plan-NeoFluar objective. Fura-2 AM-loaded cells were excited by wavelengths of 340 and 380 nm and the fluorescence emission, detected at 450–550 nm, was computed into relative ratio units (F_{340}/F_{380}).

Statistics

Where applicable, statistical errors of averaged data are given as means ± S.E.M. with n determinations and statistical significance assessed by Student's t test.

Results

Properties of non-activated and LPS-exposed mouse microglia

In acutely isolated brain slices, resting microglia are initially highly ramified and transform to amoeboid-like morphology within several hours (Stence *et al.* 2001). Here we studied shape and size of microglial cells harvested and replated from a primary coculture with astrocytes. The subcultured microglia exhibited either a ramified, rod-shaped appearance or a 'fried egg'-shaped morphology (Fig. 1*A*, left and right, respectively). Some of the cells showed a more round intermediate morphology, but with clear ramification (Fig. 1*A*, middle) and were therefore classified as ramified cells. From day 1 to day 7 after subculturing, about 90% of the cells represented the ramified and 10% the 'fried-egg'-shaped type (Fig. 1*B*). The cell membrane capacitance, which is proportional to cell surface area, was on average 12 ± 0.6 pF ($n = 76$) at day 1 and did not change significantly during the first 4 days. Thereafter the cell capacitance increased to 18.1 ± 1 pF ($n = 38$) at day 6 and 17.5 ± 1 pF ($n = 35$) at

day 7 (Fig. 1*D*). After adding 1 μg ml^{-1} lipopolysaccharide (LPS), a widely used activator of microglial cells, 34% of the cells revealed a 'fried egg'-shaped morphology already within 3 h. Within 48 h, the ratio of cell types completely reversed to just 6% ramified and 94% 'fried egg'-shaped cells (see Fig. 1*C*). The cell size increased to 23 ± 0.6 pF ($n = 155$) after 24 h and to 43.9 ± 2.6 pF ($n = 43$) after 48 h of incubation with LPS (Fig. 1*E*). Since LPS experiments were performed later than 3 days after harvest, control cells not exposed to LPS (Fig. 1*C* and *E*) represent the average data from day 3 to day 7. Bath application of 1 μg ml^{-1} LPS induced a prolonged Ca^{2+} signal (Fig. 1*F*) that set in after a marked delay of 40–50 min. After 3 h, intracellular Ca^{2+} concentration reached basic levels again, but further decreased significantly and reached a minimum after 12 h before settling in to values slightly higher than before LPS application (Fig. 1*G*).

LPS-dependent down- and up-regulation of I_{IRK} and I_{DRK}

The delayed outward rectifier (DRK) and inward rectifier (IRK) potassium channels are the dominant and best-studied ion channels in cultured microglial cells. Their down- and up-regulation often is used as a marker for the microglial activation status (Norenberg *et al.* 1994; Eder, 1998; Walz & Bekar, 2001). We determined the changes of inward and outward potassium currents of subcultured microglia over a period of 1–7 days after harvest and 3–48 h after incubation and activation with 1 μg ml^{-1} LPS. On the first day after harvest, 2.8 ± 2.8% of the cells revealed expression of I_{IRK} only, 26.1 ± 5.7% expressed I_{DRK} only, and a majority of 71.1 ± 7.4% showed both types of potassium currents ($n = 4$ coverslips with 36 cells; Fig. 2*A*). Figure 2*C–E* shows sample current–voltage (I–V) relationships of microglial

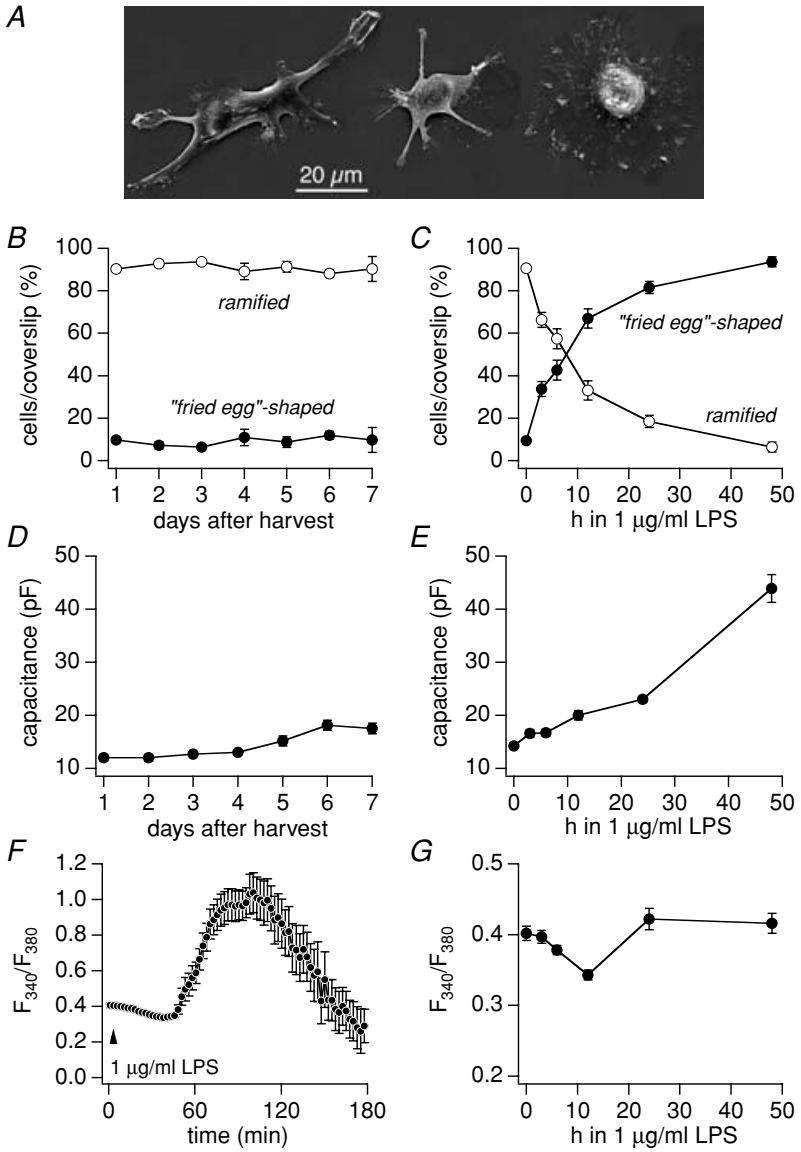

Figure 1. Morphology, cell size and $[Ca^{2+}]_i$
A, composite image of scanning electron micrographs of microglial cells at various stages of activation with 1 μg ml^{-1} LPS from non-activated (left cell, arborized) to fully activated (right cell, 'fried egg'-shaped). *B* and *C*, percentage of ramified (e, ± S.E.M.) and 'fried egg'-shaped (●, ± S.E.M.) cells per coverslip depending on time in subculture (*B*, day 1 $n = 12$, 2 $n = 10$, 3 $n = 9$, 4 $n = 5$, 5 $n = 5$, 6 $n = 8$, 7 $n = 5$ coverslips, 2142 cells) and incubation time in 1 μg ml^{-1} LPS (*C*, 0 h $n = 32$, 3 h $n = 6$, 6 h $n = 8$, 12 h $n = 4$, 24 h $n = 9$, 48 h $n = 8$ coverslips, 2211 cells). *D* and *E*, cell capacitance (in pF, ± S.E.M.) of microglial cells depending on time in subculture (*D*, day 1 $n = 76$, 2 $n = 63$, 3 $n = 110$, 4 $n = 117$, 5 $n = 35$, 6 $n = 38$, 7 $n = 35$ cells) and incubation time in 1 μg ml^{-1} LPS (*E*, 0 h $n = 335$, 3 h $n = 40$, 6 h $n = 49$, 12 h $n = 29$, 24 h $n = 155$, 48 h $n = 43$ cells). The controls (0 h LPS) in *C* and *E* represent the average data from day 3 to day 7 in *B* and *D*, respectively. *F* and *G*, intracellular Ca^{2+} changes (F_{340}/F_{380}) during the first 3 h (*F*, $n = 22$, 2 coverslips) and basic internal Ca^{2+} up to 48 h (*G*) after incubation with 1 μg ml^{-1} LPS. (*G*, 0 h $n = 47$, 3 h $n = 57$, 6 h $n = 78$, 12 h $n = 54$, 24 h $n = 26$, 48 h $n = 45$).

cells expressing I_{IRK} only (Fig. 2*C*), I_{DRK} only (Fig. 2*D*), or both I_{IRK} plus I_{DRK} (Fig. 2*E*). During the first 4 days in culture, the percentage of cells showing I_{IRK} only increased dramatically to $58.2 \pm 15.2\%$ ($n = 4$ coverslips with 32 cells) at the expense of cells expressing I_{DRK} only (0%) or $I_{IRK+DRK}$ ($41.8 \pm 15.2\%$). These relative proportions remained stable even after 7 days ($n = 3$ coverslips with 19 cells; Fig. 2*A*). With respect to average current amplitudes, I_{DRK} strongly decreased from 25.9 ± 3.4 pA pF^{-1} ($n = 36$) at day 1 to 5.2 ± 0.9 pA pF^{-1} ($n = 18$) at day 7, whereas I_{IRK} increased from 15.5 ± 2.2 pA pF^{-1} ($n = 36$) at day 1 to 27.7 ± 4.1 pA pF^{-1} ($n = 18$) at day 7 (Fig. 2*F*).

Since the most dramatic changes in potassium currents took place from day 1 to day 3, further experiments investigating early effects of LPS induction were performed on microglial cells at least 3 days in subculture. For these experiments, the unstimulated control data in Fig. 2*B* and *G* represent the average of data from day 3 to day 7. Within just 3 h, exposure of cells to 1 μg ml^{-1} LPS dramatically changed the ratio between cells expressing I_{IRK} only, I_{DRK} only and $I_{IRK+DRK}$ (see Fig. 2*B*). After 6 h of LPS exposure, the number of cells revealing $I_{IRK+DRK}$ more than doubled to $87.5 \pm 5.1\%$, cells showing I_{DRK} increased about 4-fold to $12.5 \pm 5.1\%$ and at the same time, none of the cells expressed I_{IRK} ($n = 4$ coverslips with 28 cells; Fig. 2*B*). However, within 48 h of LPS exposure the percentage of cells expressing I_{IRK} only recovered to $30.3 \pm 15.1\%$, cells presenting $I_{IRK+DRK}$ to $66 \pm 13\%$ and cells with I_{DRK} only to $3.7 \pm 3.7\%$ ($n = 3$ coverslips with 28 cells; Fig. 2*B*).

Acute LPS exposure not only affected potassium channel expression levels, but also their current amplitudes. I_{DRK} significantly increased and reached its peak after 6 h of exposure to 1 μg ml^{-1} LPS (43.9 ± 5.8 pA pF^{-1}, $n = 27$), before leveling off to control values again after 24 h of LPS exposure (10 ± 2.3 pA pF^{-1}, $n = 28$; Fig. 2*G*). In contrast, the current size of I_{IRK} gradually decreased from control levels of 22.2 ± 1.5 pA pF^{-1} ($n = 123$) to 5.6 ± 0.6 pA pF^{-1} ($n = 28$) after 24 h of incubation with LPS (Fig. 2*G*).

LPS-dependent down-regulation of I_{CRAC}

Ca^{2+} release from intracellular stores plays a critical role in intracellular signalling in many cell types. In non-excitable cells, depletion of stores activates store-operated (capacitative) Ca^{2+} entry (SOCE) to induce cellular responses and refill the Ca^{2+} stores (Putney, 1986). The calcium release-activated calcium current (I_{CRAC}) (Hoth & Penner, 1992) is the best-characterized SOCE current and the main Ca^{2+} influx pathway in immunocompetent cells such as T-lymphocytes and mast

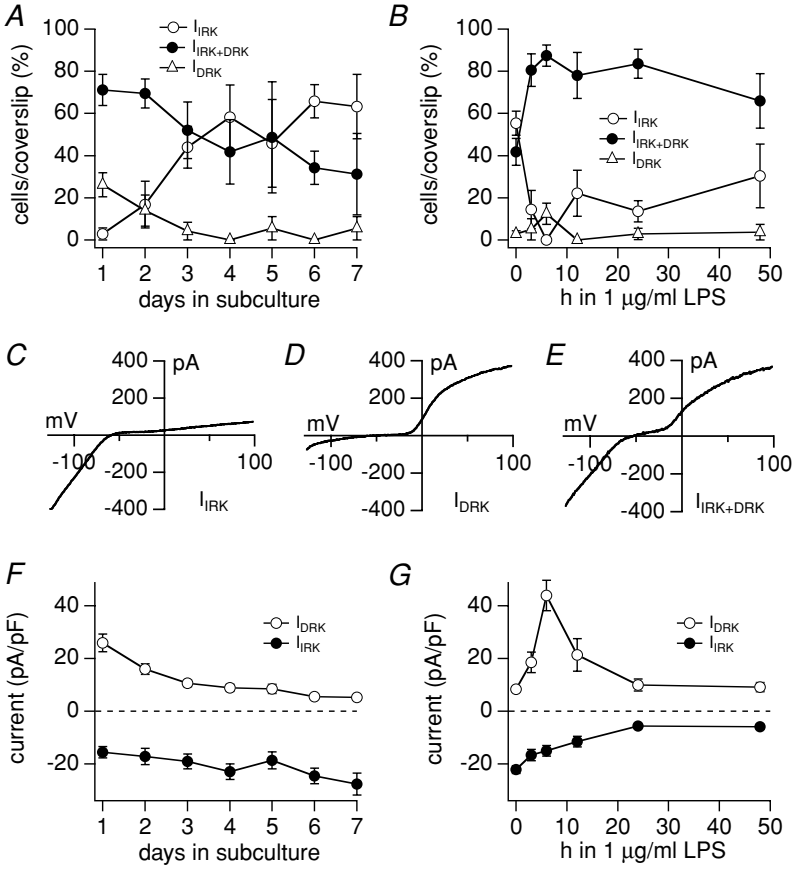

Figure 2. I_{IRK} and I_{DRK}
A and *B*, percentage of microglial cells in culture showing just I_{IRK} (e, ± S.E.M.), just I_{DRK} (△, ± S.E.M.) or $I_{IRK+DRK}$ (●, ± S.E.M.) depending on time in subculture (*A*, day 1 $n = 4$, 2 $n = 3$, 3 $n = 4$, 4 $n = 4$, 5 $n = 2$, 6 $n = 3$, 7 $n = 3$ coverslips, 183 cells) and incubation time in 1 μg ml^{-1} LPS (*B*, 0 h $n = 16$, 3 h $n = 4$, 6 h $n = 4$, 12 h $n = 2$, 24 h $n = 4$, 48 h $n = 3$ coverslips, 247 cells). *C*, *D* and *E*, typical current–voltage relationships (*I–V*) of whole-cell currents in microglial cells revealing just I_{IRK} (*C*), just I_{DRK} (*D*) and both, $I_{IRK+DRK}$ (*E*). *F* and *G*, average inward (IRK, ●, ± S.E.M.) and outward (DRK, e, ± S.E.M.) currents (in pA pF^{-1}) measured at −110 and +80 mV, respectively, of microglial cells depending on time in subculture (*F*, day 1 $n = 36$, 2 $n = 22$, 3 $n = 37$, 4 $n = 32$, 5 $n = 17$, 6 $n = 19$, day 7 $n = 18$ cells) and (*G*) incubation time in 1 μg ml^{-1} LPS (circles, 0 h $n = 123$, 3 h $n = 18$, 6 h $n = 27$, 12 h $n = 15$, 24 h $n = 28$, 48 h $n = 25$ cells). The controls (0 h LPS) in *B* and *G* represent the average data from day 3 to day 7 in *A* and *F*, respectively.

cells, but little is known about CRAC in microglial cells. We measured IP_3-induced CRAC currents in non-stimulated microglial cells over 1–7 days in subculture and during a period of 3–48 h of exposure to 1 μg ml^{-1} LPS. Figure 3*A* shows the average development of I_{CRAC} over time, normalized to cell capacitance, in microglia from day 1, 3 and 6 after replating and subculturing. The normalized amplitude of CRAC currents, measured at its plateau phase after 150–200 s into the experiment, ranged between 1.2 ± 0.13 pA pF^{-1} ($n = 11$, day 2) to 1.29 ± 0.08 pA pF^{-1} ($n = 12$, day 4), and did not change significantly during the 7 days in subculture (Fig. 3*A* and *B*). However, after exposure to 1 μg ml^{-1} LPS, current sizes of I_{CRAC} decreased with time of incubation from a control level (mean amplitude of I_{CRAC} from day 3 to day 7) of 1.25 ± 0.04 pA pF^{-1} ($n = 60$, set as 100%) to about 58% (0.73 ± 0.11 pA pF^{-1}, $n = 7$) within 12 h and further to 41% (0.51 ± 0.06 pA pF^{-1}, $n = 11$) after 48 h of exposure (Fig. 3*C* and *D*). Figure 3*E* shows the typical inward rectifying average *I–V* relationships of leak-subtracted CRAC currents after 100 s into the experiment from unstimulated control cells and cells exposed to LPS (1 μg ml^{-1}) for 24 h and 48 h.

Microglia express Ca^{2+}-activated TRPM4-like currents

Ca^{2+}-activated non-selective cation channels, like the melastatin-related transient receptor potential channels TRPM4 and TRPM5, are widely expressed and proposed to be involved in membrane depolarization (Launay *et al.* 2002; Prawitt *et al.* 2003; Guinamard *et al.* 2004). In the present study we show that perfusing microglial cells with increasing intracellular Ca^{2+} concentrations through the patch pipette, recruits a TRPM4-like current in non-activated as well as LPS-induced (24 h exposure) cells in a dose-dependent manner (see Fig. 4*A* and *C*). The dose–response curve calculated for the inward current at −80 mV yields an EC_{50} of 1.2 μM Ca^{2+} for control and 1.3 μM Ca^{2+} for 24 h LPS-exposed microglial cells (Fig. 4*C*). As seen with TRPM4 (Cheng *et al.* 2007), the Ca^{2+}-activated current in microglia (Fig. 4*A*) developed in parallel with an increase in cell

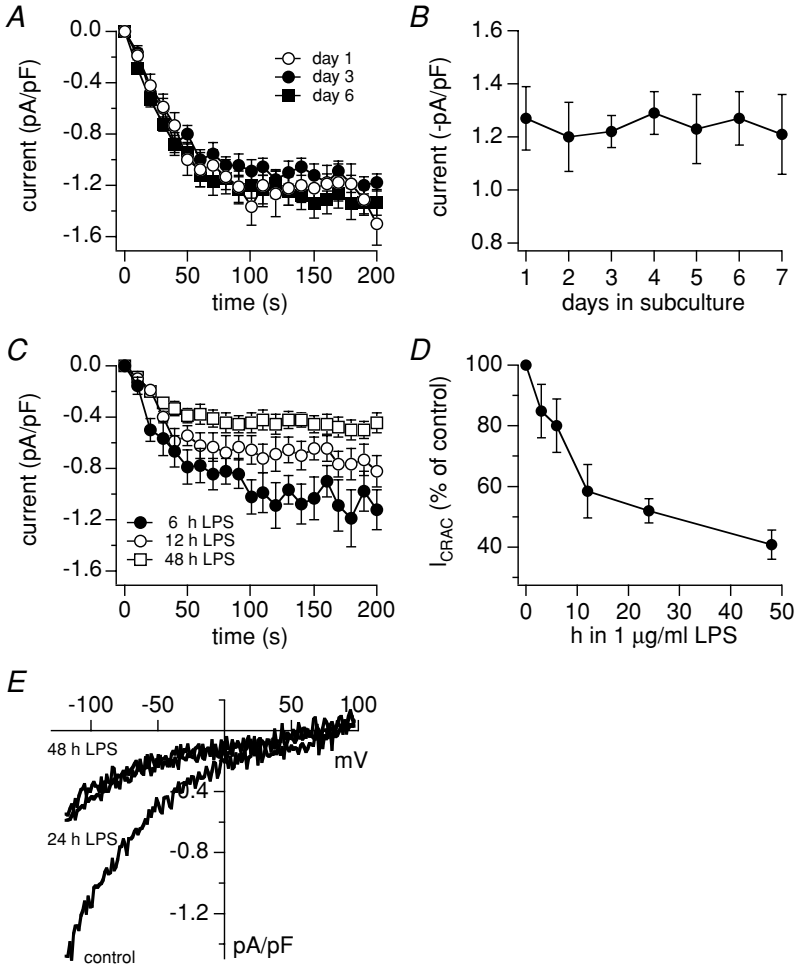

Figure 3. I_{CRAC}
A, average membrane current (I_{CRAC}, in pA pF^{-1}) measured at −110 mV 0–200 s after break-in from cultured microglial cells at day 1 (e, $n = 14$, ± S.E.M.), day 3 (●, $n = 14$, ± S.E.M.) and day 6 (■, $n = 14$, ± S.E.M.) in subculture, and *C*, after 6 h (●, $n = 8$, ± S.E.M.), 12 h (e, $n = 8$, ± S.E.M.) and 48 h (□, $n = 11$, ± S.E.M.) incubation in 1 μg ml^{-1} LPS. *B*, average I_{CRAC} amplitude (in −pA pF^{-1}), measured at the plateau current (150 s to 200 s), in dependency of time in subculture (day 1 $n = 13$, 2 $n = 11$, 3 $n = 14$, 4 $n = 12$, 5 $n = 12$, 6 $n = 15$, 7 $n = 7$ cells). *D*, I_{CRAC} (current in percentage of control ± S.E.M.) after 3 h ($n = 8$), 6 h ($n = 7$), 12 h ($n = 7$), 24 h ($n = 9$), and 48 h ($n = 11$) incubation with 1 μg ml^{-1} LPS. *E*, averaged current–voltage relationships (*I–V*s) of whole-cell currents after 100 s into the experiment measured from a resting (control, $n = 8$), a 24 h ($n = 8$) and a 48 h ($n = 10$) activated microglial cell. The control (100%, 0 h LPS) in *D* represents the average data from day 3 to day 7 in *B*.

capacitance (Fig. 4*B*), indicating that a proportion of channels might be recruited to the plasma membrane through exocytosis. The dose–response for inward and outward (data not shown) currents did not show any significant difference between non-activated and 24 h LPS-exposed microglial cells. However, 1.7 μM intracellular Ca^{2+} induced a faster recruitment of the TRPM4-like current in 24 h LPS-activated cells (see Fig. 4*A*). In addition, higher concentrations of Ca^{2+} (see Fig. 4*A* and 40 μM) resulted in a slightly larger outward current in non-activated (618 ± 55 pA pF^{-1}, $n = 19$) compared with 24 h LPS-exposed microglia (520 ± 96 pA pF^{-1}, $n = 7$). As the inward current revealed the same amplitude for control (375 ± 52 pA pF^{-1}, $n = 19$) and LPS-activated cells (377 ± 68 pA pF^{-1}, $n = 7$; see Fig. 4*A* and *C*) this results in a slightly stronger outward rectification of the TRPM4-like current in non-activated migroglial cells. Figure 4*D* shows the average *I–V* relationships of TRPM4-like currents induced by 1.7 μM intracellular Ca^{2+} in control ($n = 9$) and 24 h LPS-exposed ($n = 9$) microglial cells after 100 s and 350 s into the experiment.

Discussion

Character of non-activated microglial cells in culture

In the present study more than 90% of the mouse microglial cells appeared in a ramified, rod- or round-shaped morphology from day 1 to day 7 after harvest from an astrocyte coculture and the shape of the cells remained relatively stable. Resting microglia *in vivo* are thought to primarily express inward rectifying potassium currents (I_{IRK}) and no significant delayed outward rectifying potassium currents (I_{DRK}), increasing the expression of I_{DRK} in favour of I_{IRK} upon activation (Norenberg *et al.* 1994; Eder, 1998; Walz & Bekar, 2001). In our cultures, the initial expression pattern of potassium currents revealed that the majority of cells expressed both types of currents and about some 30% of cells had only I_{DRK}, indicating that the microglia were already somewhat preactivated in the astrocyte coculture (Schmidtmayer *et al.* 1994) and/or the harvesting procedure induced some activation. We suspect that serum levels are an important factor, since initial experiments in which we kept the levels of FBS at 10% in both co- and subculture, most of the cells showed already significant signs of activation such as amoeboid 'fried egg'-shaped morphology, often with prominent I_{DRK} (data not shown). However, coculturing cells with 10% FBS in basal modified Eagle's medium (BME) and reducing FBS to 5% in the subculture improved the yield of resting cells and most microglia were ramified rod-shaped within 3 days; most cells had little or no I_{DRK} but prominent I_{IRK}, indicating largely resting cultured microglia (Kettenmann *et al.* 1990, 1993). In contrast, Eder *et al.* (1999) and Nakamura *et al.* (1999) obtained amoeboid-shaped microglia using Dulbecco's modified Eagle's medium (DMEM) plus 10% FBS for microglia/astrocyte coculture and DMEM plus 10% or 2% FBS for the subculture (Eder *et al.* 1999; Nakamura *et al.* 1999). These cells revealed prominent I_{IRK} but no I_{DRK} (Eder *et al.* 1999). Lombardi *et al.* (2003) used BME instead of DMEM under serum-free conditions (BME also lacks L-glycine (Gly) and L-serine (Ser)). Under Gly–Ser-free serum-free conditions, microglia displayed a round morphology, whereas in the presence of 5 μM Gly

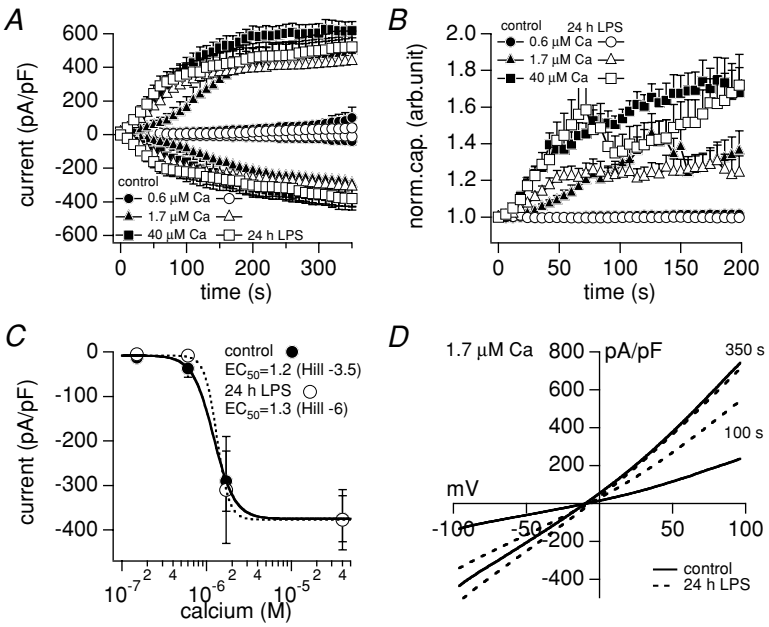

Figure 4. Calcium-activated (TRPM4-like) current
A, average inward and outward currents (in pA pF^{-1}) measured for 350 s, and *B*, normalized cell capacitance measured for 200 s after break-in from resting (filled) and activated (24 h 1 μg ml^{-1} LPS, open) microglial cells with 0.6 μM (circles, $n = 7/5$, ± S.E.M.), 1.7 μM (triangles, $n = 13/10$, ± S.E.M.) and 40 μM (squares, $n = 19/7$, ± S.E.M.) free calcium ($[Ca^{2+}]_i$) in the patch pipette. *C*, plateau inward currents (in pA pF^{-1}) after 350 s *versus* log $[Ca^{2+}]_i$ of resting (●) and activated (24 h 1 μg ml^{-1} LPS, ⁽ᵉ⁾) microglial cells. The sigmoidal fits of the inward current amplitudes revealed an EC_{50} of 1.2 μM Ca^{2+} (Hill coefficient = −3.5) for resting and 1.3 μM Ca^{2+} (Hill = −6) for activated microglial cells. *D*, average current–voltage relationships (*I–V*s) of whole-cell currents (in pA pF^{-1}) activated by 1.7 μM internal Ca^{2+} from resting (control, continuous traces, $n = 9$) and activated (24 h 1 μg ml^{-1} LPS, dotted traces, $n = 9$) microglial cells at 100 s and 350 s into the experiment.

and 25 μM Ser they revealed ramifications (Lombardi *et al.* 2003). These and our results show that the morphological and electrophysiological character of cultured microglial cells depend on the environmental condition, and the electrophysiological properties do not necessarily correlate completely with the morphology in culture.

Resting microglia *in vivo* are highly ramified and convert into amoeboid macrophage-like cells when activated (Thomas, 1992; Vilhardt, 2005). As tissue preparations represent traumatic injuries that result in activated microglia, physiological aspects of resting microglial function and early activation *in vivo* remains largely elusive. The probably closest representation of truly resting microglia *in vivo* are ramified microglial cells found in acutely isolated brain slices. A few hours after preparation, microglial cells of rat hippocampal brain slices change their morphology from ramified to amoeboid (Stence *et al.* 2001). Interestingly, and in contrast to cultured cells, microglia in rat brain slices revealed almost no inward and voltage-gated outward potassium currents (Boucsein *et al.* 2000). Within 12 h after facial nerve axotomy, microglia in the facial nucleus expressed a prominent I_{IRK} and thus acquired the physiological properties of cultured microglial cells. Within 24 h of axotomy, the cells expressed I_{DRK}, which is typical for lipopolysaccharide (LPS)-exposed cultured microglia. Similar results have been obtained after a permanent middle cerebral artery occlusion (MCAO) in the rat brain (Lyons *et al.* 2000). It thus appears that the activation of microglial cells *in vivo* proceeds in two steps, first characterized by the expression of I_{IRK} and later by I_{DRK}. Since cultured non-activated microglial cells reveal almost exclusively I_{IRK} they represent a similar physiology as the early activated stage (Boucsein *et al.* 2000; Lyons *et al.* 2000), which is also similar to the highly motile microglia invading the brain in early development, as these cells also express just I_{IRK} (Brockhaus *et al.* 1993). Thus, cultured microglial cells might represent an early intermediate stage between resting and activated microglia that still allows the study of further microglia activation.

Potassium currents (I_{IRK} and I_{DRK}) after LPS exposure

Microglial cells appear in different shapes and express a distinct pattern of ion channels according to their status of activation. In our study, non-activated cultured microglia appeared in a ramified, rod- or round-shaped morphology with prominent I_{IRK}. After exposure to 1 μg ml^{-1} LPS, cells responded with an increase in cell capacitance (surface area) and exhibited an amoeboid, 'fried egg'-shaped morphology (see Fig. 1*C* and *D*). While I_{IRK} constantly decreased, I_{DRK} reached maximal expression within 6 h but decreased thereafter again (see Fig. 2*B* and *G*). This result is in agreement with the general consensus that resting cultured microglia primarily express I_{IRK} and recruit I_{DRK} after exposure to LPS (Kettenmann *et al.* 1990, 1993; Norenberg *et al.* 1992, 1994; Illes *et al.* 1996; McLarnon *et al.* 1997; Draheim *et al.* 1999). The I_{IRK} is suggested to be of the Kir2.1-like subtype (Newell & Schlichter, 2005) and LPS-activated microglia express mRNA and proteins for the delayed outward rectifier potassium channels Kv1.3 and Kv1.5 (Khanna *et al.* 2001). While pharmacological evidence indicates that the channel might be of the Kv1.3 subtype (Pyo *et al.* 1997; Visentin & Levi, 1998; Cayabyab *et al.* 2000; Khanna *et al.* 2001), immunological data by Pyo *et al.* (1997) suggested that the LPS-induced outward current is probably due to the Kv1.5 subtype and more recent studies revealed that LPS-induced I_{DRK} is reduced in Kv1.5$^{-/-}$ knock-out mice. Since K^+ currents in antisense oligonucleotide-treated cultured mouse microglial cells are affected (Pannasch *et al.* 2006), it seems possible that both Kv1.5 as well as Kv1.3 might be expressed in microglia.

Less is known about the physiological functions of I_{IRK} and I_{DRK} in microglial cells. I_{DRK} seems to be somehow correlated to NO release, since knock-out or block of Kv1.5, but not Kv1.3, resulted in a significant decrease in LPS-induced NO release in culture (Pyo *et al.* 1997; Pannasch *et al.* 2006), and Kv1.5 expression *in vivo* precedes the expression of inducible nitric oxide synthase (iNOS) (Jou *et al.* 1998). In addition, the Kv1.3 inhibitor agitoxin-2 reduced the microglial respiratory burst, a metabolic cascade that generates antimicrobial superoxide and other reactive oxygen intermediates (Khanna *et al.* 2001). I_{IRK} and I_{DRK} are mostly discussed to stabilize the membrane potential and are involved in microglial proliferation (Chung *et al.* 1999; Kotecha & Schlichter, 1999; Eder, 2005; Pannasch *et al.* 2006). Since resting microglia *in vivo* are devoid of the potassium currents, their membrane potential is relatively positive (Boucsein *et al.* 2000). In a first step of LPS-induced activation, I_{IRK} appears (Boucsein *et al.* 2000; Lyons *et al.* 2000) and the membrane potential becomes more negative. Hence, microglia cell activation correlates with an increase of the driving force for Ca^{2+} into the cell. This also applies to non-activated microglial cells in culture, as they already express I_{IRK}. In the absence of I_{DRK}, even a small inward current can lead to a large membrane depolarization. In a second step, I_{DRK} appears in microglia *in vivo* (Boucsein *et al.* 2000; Lyons *et al.* 2000) as well as in cultured microglia (Kettenmann *et al.* 1990, 1993; Norenberg *et al.* 1992, 1994; Illes *et al.* 1996; Newell & Schlichter, 2005), stabilizing the negative membrane potential and the driving force for Ca^{2+} into the cell. Franchini *et al.* (2004) observed that inhibition of I_{IRK} with Ba^{2+} significantly reduced the Ca^{2+} influx following receptor activation (Franchini *et al.* 2004). Our results reveal that following an initial peak after 6 h of LPS exposure, the amplitude of I_{DRK} decreased again within 24 h to almost basal level. There was also

a parallel decrease in the amplitude of I_{IRK}. Both effects would favour a more depolarized membrane potential and decreased driving force for Ca^{2+} into the cell. After about 48 h, the expression pattern returned to that observed in microglia prior to LPS exposure in culture, with most cells expressing both I_{IRK} and I_{DRK}, but with relatively small amplitudes (see Fig. 2*B* and *G*). The cell shape, however, remained amoeboid. The transient increase in I_{DRK} and the associated potential for enhanced Ca^{2+} driving force into the cell indicates some importance for Ca^{2+} signalling, especially during the first 6 h after LPS-induced activation.

Time course of LPS-induced effects

Most studies in cultured microglia assess the effects of LPS 24 h or later after exposure, a time where the most prominent electrophysiological change in our study, the increase of I_{DRK}, has already declined (see Fig. 2*G*). In addition, the most prominent changes in $[Ca^{2+}]_i$ caused by LPS occur over a time window that is not typically studied by most investigations. After a delay of 40–50 min, LPS induces a prolonged increase in the intracellular Ca^{2+} levels, followed by a transient undershoot lasting several hours, before returning to normal levels (see Fig. 1*F* and *G*). Thus, our results show that the most dramatic changes in terms of basic Ca^{2+} take place in the first 3 h and in terms of potassium currents in the first 3–6 h after LPS exposure. Intracerebroventricular injection of LPS in mice induced a sharp peak of interleukin-6 (IL-6) and monocyte chemotactic protein-1 (MCP-1) production at about 4 h, returning to baseline after about 16 h (Lund *et al.* 2006). Nakamura *et al.* (1999) also reported the most dramatic production of IL-6 as well as IL-1-β and TNF-α in the first 6 h after LPS exposure (Nakamura *et al.* 1999). Interestingly, IL-6 and IL-1-β induction remained elevated, TNF-α expression declined after 12 h. These LPS-induced events thus occur in a similar time frame as I_{DRK} and the resulting increase in Ca^{2+} signalling ability seen in our study. Nakamura *et al.* (1999) also showed that LPS induced a transient change of morphology from round amoeboid to process-bearing bipolar and back to round cells, where the cells reached maximum size after 6 h and returned to baseline after 24 h (Nakamura *et al.* 1999). In contrast, we observed a continuous increase of cell capacitance and a consistent morphological change from ramified to amoeboid over a period of 48 h after LPS exposure (see Fig. 1*C* and *E*). These differences in morphology and time course might be due to the fact that Nakamura *et al.* (1999) studied rat microglial cells grown in DMEM and we studied mouse microglial cells grown in BME medium.

I_{CRAC} in cultured microglial cells

Ca^{2+} signalling is widely used as a central mechanism for numerous cellular functions in other immunocompetent cells. However, the involvement of Ca^{2+} and the role of different Ca^{2+} signalling mechanisms in microglial cells are largely unknown. Microglial cells express several receptors such as purinergic P2Y (James & Butt, 2002; McLarnon, 2005; Light *et al.* 2006), adrenergic α1 (Mori *et al.* 2002), muscarinic (Whittemore *et al.* 1993; Zhang *et al.* 1998) endothelin (Moller *et al.* 1997; McLarnon *et al.* 1999), thrombin (Moller *et al.* 2000), platelet-activating factor (Mori *et al.* 1996) and cytokine/chemokine receptors (Boddeke *et al.* 1999; Franciosi *et al.* 2002; Shideman *et al.* 2006), coupled to the second messenger inositol 1,4,5-trisphosphate (IP_3) and mediating release of Ca^{2+} from intracellular stores. Ca^{2+} release often is followed by a prolonged secondary phase that is due to store-operated (capacitative) Ca^{2+} entry (SOCE) (Putney, 1986). The best characterized SOCE current and probably the main Ca^{2+} influx pathway in immunocompetent cells is the Ca^{2+} release-activated Ca^{2+} current (I_{CRAC}) (Hoth & Penner, 1992). In microglial cells, SOCE has so far mainly been studied via Ca^{2+} imaging techniques (Toescu *et al.* 1998; Khoo *et al.* 2001; Choi *et al.* 2003), only few publications showing microglial I_{CRAC} measured with the whole-cell patch-clamp technique (Norenberg *et al.* 1997; Hahn *et al.* 2000). In the present study we show that the amplitude of I_{CRAC} in cultured microglial cells decreases significantly with time of activation and LPS exposure. In contrast to the transient increase in I_{DRK} with the peak after 6 h, I_{CRAC} continuously decreased, indicating an immediate down-regulation of Ca^{2+} influx after LPS-induced activation. This suggests that either increasing the driving force for Ca^{2+} is not the major purpose of LPS-induced increase of I_{DRK}, or I_{CRAC} is not its most important addressee. SOCE is probably the major but not the only way of Ca^{2+} influx into microglial cells. There is no evidence for voltage-gated Ca^{2+} channels in microglial cells, but they reportedly express several other Ca^{2+}-permeable ion channels such as the AMPA (α-amino-3-hydroxy-4-methyl-4-isoxazole propionate) receptor channel, a subtype of the ionotropic glutamate receptor, with a relatively low Ca^{2+} permeability (Noda *et al.* 2000), TRPM2 and TRPM7, members of the melastatin-related transient potential receptor channels (Wang *et al.* 2000; Jiang *et al.* 2003) and purinergic P2X receptors (Visentin *et al.* 1999; Wang *et al.* 2000; Farber & Kettenmann, 2006). In terms of intracellular Ca^{2+}, LPS exposure also induces Ca^{2+} transients in cultured microglial cells (see Fig. 1*F*, unidentified mechanism), possibly resulting from caffeine-sensitive Ca^{2+} release (Bader *et al.* 1994) and/or dependent on unidentified Ca^{2+} influx channels (Herms *et al.* 1997; Choi *et al.* 2002; Yi *et al.* 2005).

I_{CAN} in LPS-induced activation of cultured microglial cells

Besides voltage-gated potassium channels, other ion channels such as Ca^{2+}-activated K^+ channels (Kaushal *et al.* 2007), H^+ channels (Klee *et al.* 1998, 1999), non-selective cation channels (Schilling *et al.* 2004), and Cl^- channels (Schlichter *et al.* 1996; Eder *et al.* 1998) have also been shown to be involved in further activation or proliferation of cultured microglial cells, although their temporal expression patterns during the activation process have not yet been characterized. Our study additionally reveals a Ca^{2+}-activated TRPM4-like current in non-activated cultured mouse microglial cells. Ca^{2+}-activated cation channels such as TRPM4 and TRPM5 are widely expressed and proposed to be involved in membrane depolarization (Launay *et al.* 2002; Prawitt *et al.* 2003; Guinamard *et al.* 2004). While I_{IRK} and I_{DRK} support the driving force for Ca^{2+} through negative membrane potentials, incoming Ca^{2+} might depolarize the microglial cells via activation of the TRPM4-like current, thus reducing the driving force and regulating the Ca^{2+} influx negatively. In electrically non-excitable Jurkat T lymphocytes, suppression of TRPM4 disregulates receptor-induced Ca^{2+} oscillations leading to enhanced IL-2 production due to sustained increases in cellular Ca^{2+} levels (Launay *et al.* 2004). In microglia, however, besides a slightly faster activation and a slightly stronger outward rectification, LPS exposure did not significantly change the character or size of the Ca^{2+}-activated TRPM4-like I_{CAN}. We therefore propose that LPS-induced down-regulation of I_{IRK} and I_{CRAC} reduces the cell's capacity to produce significant Ca^{2+} influx upon receptor stimulation and results in decreased sensitivity to additional exogenous stimulation. In this scenario, I_{CAN} does not need to be affected, as its activity would automatically be adjusted due to the diminished calcium influx capacity of the cell.

The mechanism(s) of LPS-induced down-regulation of I_{IRK} and I_{CRAC} and transient up-regulation of I_{DRK} are not known yet. However, the activation of microglial Toll-like receptor-4 (TLR-4) by LPS results in the induction of an array of genes that are involved in initiation or regulation of the inflammatory response (Hoshino *et al.* 1999; Lee & Lee, 2002). LPS-induced CD40 expression involves activation of the transcription factor nuclear factor-κB (NF-κB) and signal transducer and activator of transcription 1α (STAT-1α), which is activated by the endogenous production of interferon-β (IFN-β) (Qin *et al.* 2005). The extended delayed transient Ca^{2+} increase after LPS exposure observed in this study (see Fig. 1*F*) might also be involved in nuclear gene regulation, since it is known that intracellular Ca^{2+} signals can trigger gene expression.

References

abd-el-Basset E & Fedoroff S (1995). Effect of bacterial wall lipopolysaccharide (LPS) on morphology, motility, and cytoskeletal organization of microglia in cultures. *J Neurosci Res* **41**, 222–237.

Ajmone-Cat MA, Nicolini A & Minghetti L (2003). Prolonged exposure of microglia to lipopolysaccharide modifies the intracellular signaling pathways and selectively promotes prostaglandin E2 synthesis. *J Neurochem* **87**, 1193–1203.

Bader MF, Taupenot L, Ulrich G, Aunis D & Ciesielski-Treska J (1994). Bacterial endotoxin induces $[Ca^{2+}]_i$ transients and changes the organization of actin in microglia. *Glia* **11**, 336–344.

Baker CA & Manuelidis L (2003). Unique inflammatory RNA profiles of microglia in Creutzfeldt-Jakob disease. *Proc Natl Acad Sci U S A* **100**, 675–679.

Biro T, Brodie C, Modarres S, Lewin NE, Acs P & Blumberg PM (1998). Specific vanilloid responses in C6 rat glioma cells. *Brain Res Mol Brain Res* **56**, 89–98.

Bo L, Mork S, Kong PA, Nyland H, Pardo CA & Trapp BD (1994). Detection of MHC class II-antigens on macrophages and microglia, but not on astrocytes and endothelia in active multiple sclerosis lesions. *J Neuroimmunol* **51**, 135–146.

Boddeke EW, Meigel I, Frentzel S, Gourmala NG, Harrison JK, Buttini M, Spleiss O & Gebicke-Harter P (1999). Cultured rat microglia express functional β-chemokine receptors. *J Neuroimmunol* **98**, 176–184.

Boucsein C, Kettenmann H & Nolte C (2000). Electrophysiological properties of microglial cells in normal and pathologic rat brain slices. *Eur J Neurosci* **12**, 2049–2058.

Brockhaus J, Ilschner S, Banati RB & Kettenmann H (1993). Membrane properties of ameboid microglial cells in the corpus callosum slice from early postnatal mice. *J Neurosci* **13**, 4412–4421.

Cayabyab FS, Khanna R, Jones OT & Schlichter LC (2000). Suppression of the rat microglia Kv1.3 current by src-family tyrosine kinases and oxygen/glucose deprivation. *Eur J Neurosci* **12**, 1949–1960.

Cheng H, Beck A, Launay P, Gross SA, Stokes AJ, Kinet JP, Fleig A & Penner R (2007). TRPM4 controls insulin secretion in pancreatic β-cells. *Cell Calcium* **41**, 51–61.

Choi HB, Hong SH, Ryu JK, Kim SU & McLarnon JG (2003). Differential activation of subtype purinergic receptors modulates Ca^{2+} mobilization and COX-2 in human microglia. *Glia* **43**, 95–103.

Choi HB, Khoo C, Ryu JK, van Breemen E, Kim SU & McLarnon JG (2002). Inhibition of lipopolysaccharide-induced cyclooxygenase-2, tumor necrosis factor-α and $[Ca^{2+}]_i$ responses in human microglia by the peripheral benzodiazepine receptor ligand PK11195. *J Neurochem* **83**, 546–555.

Chung S, Jung W & Lee MY (1999). Inward and outward rectifying potassium currents set membrane potentials in activated rat microglia. *Neurosci Lett* **262**, 121–124.

Conde JR & Streit WJ (2006). Microglia in the aging brain. *J Neuropathol Exp Neurol* **65**, 199–203.

del Rio Hortega P (1932). Microglia. In *Cytology and Cellular Pathology of the Nervous System*, ed.Penfield W, Vol. 2, pp. 481–534. Paul B Hoeber, New York.

Dickson DW, Mattiace LA, Kure K, Hutchins K, Lyman WD & Brosnan CF (1991). Microglia in human disease, with an emphasis on acquired immune deficiency syndrome. *Lab Invest* **64**, 135–156.

Draheim HJ, Prinz M, Weber JR, Weiser T, Kettenmann H & Hanisch UK. (1999). Induction of potassium channels in mouse brain microglia: cells acquire responsiveness to pneumococcal cell wall components during late development. *Neuroscience* **89**, 1379–1390.

Eder C (1998). Ion channels in microglia (brain macrophages). *Am J Physiol Cell Physiol* **275**, C327–C342.

Eder C (2005). Regulation of microglial behavior by ion channel activity. *J Neurosci Res* **81**, 314–321.

Eder C, Klee R & Heinemann U (1998). Involvement of stretch-activated Cl^- channels in ramification of murine microglia. *J Neurosci* **18**, 7127–7137.

Eder C, Schilling T, Heinemann U, Haas D, Hailer N & Nitsch R (1999). Morphological, immunophenotypical and electrophysiological properties of resting microglia in vitro. *Eur J Neurosci* **11**, 4251–4261.

Farber K & Kettenmann H (2005). Physiology of microglial cells. *Brain Res Brain Res Rev* **48**, 133–143.

Farber K & Kettenmann H (2006). Functional role of calcium signals for microglial function. *Glia* **54**, 656–665.

Franchini L, Levi G & Visentin S (2004). Inwardly rectifying K^+ channels influence Ca^{2+} entry due to nucleotide receptor activation in microglia. *Cell Calcium* **35**, 449–459.

Franciosi S, Choi HB, Kim SU & McLarnon JG (2002). Interferon-γ acutely induces calcium influx in human microglia. *J Neurosci Res* **69**, 607–613.

Giulian D & Baker TJ (1986). Characterization of ameboid microglia isolated from developing mammalian brain. *J Neurosci* **6**, 2163–2178.

Guinamard R, Chatelier A, Demion M, Potreau D, Patri S, Rahmati M & Bois P (2004). Functional characterization of a Ca^{2+}-activated non-selective cation channel in human atrial cardiomyocytes. *J Physiol* **558**, 75–83.

Hahn J, Jung W, Kim N, Uhm DY & Chung S (2000). Characterization and regulation of rat microglial Ca^{2+} release-activated Ca^{2+} (CRAC) channel by protein kinases. *Glia* **31**, 118–124.

Herms JW, Madlung A, Brown DR & Kretzschmar HA (1997). Increase of intracellular free Ca^{2+} in microglia activated by prion protein fragment. *Glia* **21**, 253–257.

Hoffmann A, Kann O, Ohlemeyer C, Hanisch UK & Kettenmann H (2003). Elevation of basal intracellular calcium as a central element in the activation of brain macrophages (microglia): suppression of receptor-evoked calcium signaling and control of release function. *J Neurosci* **23**, 4410–4419.

Hoshino K, Takeuchi O, Kawai T, Sanjo H, Ogawa T, Takeda Y, Takeda K & Akira S (1999). Cutting edge: Toll-like receptor 4 (TLR4)-deficient mice are hyporesponsive to lipopolysaccharide: evidence for TLR4 as the Lps gene product. *J Immunol* **162**, 3749–3752.

Hoth M & Penner R (1992). Depletion of intracellular calcium stores activates a calcium current in mast cells. *Nature* **355**, 353–356.

Illes P, Norenberg W & Gebicke-Haerter PJ (1996). Molecular mechanisms of microglial activation. B. Voltage- and purinoceptor-operated channels in microglia. *Neurochem Int* **29**, 13–24.

Jack C, Ruffini F, Bar-Or A & Antel JP (2005). Microglia and multiple sclerosis. *J Neurosci Res* **81**, 363–373.

James G & Butt AM (2002). P2Y and P2X purinoceptor mediated Ca^{2+} signalling in glial cell pathology in the central nervous system. *Eur J Pharmacol* **447**, 247–260.

Jiang X, Newell EW & Schlichter LC (2003). Regulation of a TRPM7-like current in rat brain microglia. *J Biol Chem* **278**, 42867–42876.

Jou I, Pyo H, Chung S, Jung SY, Gwag BJ & Joe EH (1998). Expression of Kv1.5 K^+ channels in activated microglia in vivo. *Glia* **24**, 408–414.

Kaushal V, Koeberle PD, Wang Y & Schlichter LC (2007). The Ca^{2+}-activated K^+ channel KCNN4/KCa3.1 contributes to microglia activation and nitric oxide-dependent neurodegeneration. *J Neurosci* **27**, 234–244.

Kershbaum J (1939). Genesis of microglia in the human brain. *Arch Neurol Psychiatry* **41**, 24–50.

Kettenmann H, Banati R & Walz W (1993). Electrophysiological behavior of microglia. *Glia* **7**, 93–101.

Kettenmann H, Hoppe D, Gottmann K, Banati R & Kreutzberg G (1990). Cultured microglial cells have a distinct pattern of membrane channels different from peritoneal macrophages. *J Neurosci Res* **26**, 278–287.

Khanna R, Roy L, Zhu X & Schlichter LC (2001). K^+ channels and the microglial respiratory burst. *Am J Physiol Cell Physiol* **280**, C796–C806.

Khoo C, Helm J, Choi HB, Kim SU & McLarnon JG (2001). Inhibition of store-operated Ca^{2+} influx by acidic extracellular pH in cultured human microglia. *Glia* **36**, 22–30.

Klee R, Heinemann U & Eder C (1998). Changes in proton currents in murine microglia induced by cytoskeletal disruptive agents. *Neurosci Lett* **247**, 191–194.

Klee R, Heinemann U & Eder C (1999). Voltage-gated proton currents in microglia of distinct morphology and functional state. *Neuroscience* **91**, 1415–1424.

Kloss CU, Bohatschek M, Kreutzberg GW & Raivich G (2001). Effect of lipopolysaccharide on the morphology and integrin immunoreactivity of ramified microglia in the mouse brain and in cell culture. *Exp Neurol* **168**, 32–46.

Kotecha SA & Schlichter LC (1999). A Kv1.5 to Kv1.3 switch in endogenous hippocampal microglia and a role in proliferation. *J Neurosci* **19**, 10680–10693.

Launay P, Cheng H, Srivatsan S, Penner R, Fleig A & Kinet JP (2004). TRPM4 regulates calcium oscillations after T cell activation. *Science* **306**, 1374–1377.

Launay P, Fleig A, Perraud AL, Scharenberg AM, Penner R & Kinet JP (2002). TRPM4 is a Ca^{2+}-activated nonselective cation channel mediating cell membrane depolarization. *Cell* **109**, 397–407.

Lawson LJ, Perry VH, Dri P & Gordon S (1990). Heterogeneity in the distribution and morphology of microglia in the normal adult mouse brain. *Neuroscience* **39**, 151–170.

Lee SJ & Lee S (2002). Toll-like receptors and inflammation in the CNS. *Curr Drug Targets Inflamm Allergy* **1**, 181–191.

Light AR, Wu Y, Hughen RW & Guthrie PB (2006). Purinergic receptors activating rapid intracellular Ca increases in microglia. *Neuron Glia Biol* **2**, 125–138.

Lombardi VR, Etcheverria I, Fernandez-Novoa L & Cacabelos R (2003). In vitro regulation of rat derived microglia. *Neurotox Res* **5**, 201–212.

Lund S, Christensen KV, Hedtjarn M, Mortensen AL, Hagberg H, Falsig J, Hasseldam H, Schrattenholz A, Porzgen P & Leist M (2006). The dynamics of the LPS triggered inflammatory response of murine microglia under different culture and in vivo conditions. *J Neuroimmunol* **180**, 71–87.

Lyons SA, Pastor A, Ohlemeyer C, Kann O, Wiegand F, Prass K, Knapp F, Kettenmann H & Dirnagl U (2000). Distinct physiologic properties of microglia and blood-borne cells in rat brain slices after permanent middle cerebral artery occlusion. *J Cereb Blood Flow Metab* **20**, 1537–1549.

McGeer PL, Itagaki S, Boyes BE & McGeer EG (1988). Reactive microglia are positive for HLA-DR in the substantia nigra of Parkinson's and Alzheimer's disease brains. *Neurology* **38**, 1285–1291.

McGeer PL & McGeer EG (1995). The inflammatory response system of brain: implications for therapy of Alzheimer and other neurodegenerative diseases. *Brain Res Brain Res Rev* **21**, 195–218.

McLarnon JG (2005). Purinergic mediated changes in Ca^{2+} mobilization and functional responses in microglia: effects of low levels of ATP. *J Neurosci Res* **81**, 349–356.

McLarnon JG, Wang X, Bae JH & Kim SU (1999). Endothelin-induced changes in intracellular calcium in human microglia. *Neurosci Lett* **263**, 9–12.

McLarnon JG, Xu R, Lee YB & Kim SU (1997). Ion channels of human microglia in culture. *Neuroscience* **78**, 1217–1228.

Meda L, Cassatella MA, Szendrei GI, Otvos L Jr, Baron P, Villalba M, Ferrari D & Rossi F (1995). Activation of microglial cells by β-amyloid protein and interferon-γ. *Nature* **374**, 647–650.

Moller T & Hanisch UK & Ransom BR (2000). Thrombin-induced activation of cultured rodent microglia. *J Neurochem* **75**, 1539–1547.

Moller T, Kann O, Prinz M, Kirchhoff F, Verkhratsky A & Kettenmann H (1997). Endothelin-induced calcium signaling in cultured mouse microglial cells is mediated through ETB receptors. *Neuroreport* **8**, 2127–2131.

Mori K, Ozaki E, Zhang B, Yang L, Yokoyama A, Takeda I, Maeda N, Sakanaka M & Tanaka J (2002). Effects of norepinephrine on rat cultured microglial cells that express α1, α2, β1 and β2 adrenergic receptors. *Neuropharmacology* **43**, 1026–1034.

Mori M, Aihara M, Kume K, Hamanoue M, Kohsaka S & Shimizu T (1996). Predominant expression of platelet-activating factor receptor in the rat brain microglia. *J Neurosci* **16**, 3590–3600.

Nakamura Y, Si QS & Kataoka K (1999). Lipopolysaccharide-induced microglial activation in culture: temporal profiles of morphological change and release of cytokines and nitric oxide. *Neurosci Res* **35**, 95–100.

Newell EW & Schlichter LC (2005). Integration of K^+ and Cl^- currents regulate steady-state and dynamic membrane potentials in cultured rat microglia. *J Physiol* **567**, 869–890.

Noda M, Nakanishi H, Nabekura J & Akaike N (2000). AMPA-kainate subtypes of glutamate receptor in rat cerebral microglia. *J Neurosci* **20**, 251–258.

Norenberg W, Cordes A, Blohbaum G, Frohlich R & Illes P (1997). Coexistence of purino- and pyrimidinoceptors on activated rat microglial cells. *Br J Pharmacol* **121**, 1087–1098.

Norenberg W, Gebicke-Haerter PJ & Illes P (1992). Inflammatory stimuli induce a new K^+ outward current in cultured rat microglia. *Neurosci Lett* **147**, 171–174.

Norenberg W, Gebicke-Haerter PJ & Illes P (1994). Voltage-dependent potassium channels in activated rat microglia. *J Physiol* **475**, 15–32.

Pannasch U, Farber K, Nolte C, Blonski M, Yan Chiu S, Messing A & Kettenmann H (2006). The potassium channels Kv1.5 and Kv1.3 modulate distinct functions of microglia. *Mol Cell Neurosci* **33**, 401–411.

Persson M, Brantefjord M, Hansson E & Ronnback L (2005). Lipopolysaccharide increases microglial GLT-1 expression and glutamate uptake capacity in vitro by a mechanism dependent on TNF-α. *Glia* **51**, 111–120.

Prawitt D, Monteilh-Zoller MK, Brixel L, Spangenberg C, Zabel B, Fleig A & Penner R (2003). TRPM5 is a transient Ca^{2+}-activated cation channel responding to rapid changes in $[Ca^{2+}]_i$. *Proc Natl Acad Sci U S A* **100**, 15166–15171.

Putney JW Jr (1986). A model for receptor-regulated calcium entry. *Cell Calcium* **7**, 1–12.

Pyo H, Chung S, Jou I, Gwag B & Joe EH (1997). Expression and function of outward K^+ channels induced by lipopolysaccharide in microglia. *Mol Cells* **7**, 610–614.

Qin H, Wilson CA, Lee SJ, Zhao X & Benveniste EN (2005). LPS induces CD40 gene expression through the activation of NF-γB and STAT-1α in macrophages and microglia. *Blood* **106**, 3114–3122.

Rock RB, Gekker G, Hu S, Sheng WS, Cheeran M, Lokensgard JR & Peterson PK (2004). Role of microglia in central nervous system infections. *Clin Microbiol Rev* **17**, 942–964.

Sargsyan SA, Monk PN & Shaw PJ (2005). Microglia as potential contributors to motor neuron injury in amyotrophic lateral sclerosis. *Glia* **51**, 241–253.

Sasaki A, Hirato J & Nakazato Y (1993). Immunohistochemical study of microglia in the Creutzfeldt-Jakob diseased brain. *Acta Neuropathol* **86**, 337–344.

Schilling T, Lehmann F, Ruckert B & Eder C (2004). Physiological mechanisms of lysophosphatidylcholine-induced de-ramification of murine microglia. *J Physiol* **557**, 105–120.

Schlichter LC, Sakellaropoulos G, Ballyk B, Pennefather PS & Phipps DJ (1996). Properties of K^+ and Cl^- channels and their involvement in proliferation of rat microglial cells. *Glia* **17**, 225–236.

Schmidtmayer J, Jacobsen C, Miksch G & Sievers J (1994). Blood monocytes and spleen macrophages differentiate into microglia-like cells on monolayers of astrocytes: membrane currents. *Glia* **12**, 259–267.

Shideman CR, Hu S, Peterson PK & Thayer SA (2006). CCL5 evokes calcium signals in microglia through a kinase-, phosphoinositide-, and nucleotide-dependent mechanism. *J Neurosci Res* **83**, 1471–1484.

Stence N, Waite M & Dailey ME (2001). Dynamics of microglial activation: a confocal time-lapse analysis in hippocampal slices. *Glia* **33**, 256–266.

Streit WJ, Graeber MB & Kreutzberg GW (1989). Expression of Ia antigen on perivascular and microglial cells after sublethal and lethal motor neuron injury. *Exp Neurol* **105**, 115–126.

Streit WJ, Mrak RE & Griffin WS (2004). Microglia and neuroinflammation: a pathological perspective. *J Neuroinflammation* **1**, 14.

Thomas WE (1992). Brain macrophages: evaluation of microglia and their functions. *Brain Res Brain Res Rev* **17**, 61–74.

Toescu EC, Moller T, Kettenmann H & Verkhratsky A (1998). Long-term activation of capacitative Ca^{2+} entry in mouse microglial cells. *Neuroscience* **86**, 925–935.

Vilhardt F (2005). Microglia: phagocyte and glia cell. *Int J Biochem Cell Biol* **37**, 17–21.

Visentin S & Levi G (1998). Arachidonic acid-induced inhibition of microglial outward-rectifying K^+ current. *Glia* **22**, 1–10.

Visentin S, Renzi M, Frank C, Greco A & Levi G (1999). Two different ionotropic receptors are activated by ATP in rat microglia. *J Physiol* **519**, 723–736.

Walz W & Bekar LK (2001). Ion channels in cultured microglia. *Microsc Res Tech* **54**, 26–33.

Wang X, Kim SU, van Breemen C & McLarnon JG (2000). Activation of purinergic P2X receptors inhibits P2Y-mediated Ca^{2+} influx in human microglia. *Cell Calcium* **27**, 205–212.

Wang XJ, Yan ZQ, Lu GQ, Stuart S & Chen SD (2007). Parkinson disease IgG and C5a-induced synergistic dopaminergic neurotoxicity: role of microglia. *Neurochem Int* **50**, 39–50.

Whittemore ER, Korotzer AR, Etebari A & Cotman CW (1993). Carbachol increases intracellular free calcium in cultured rat microglia. *Brain Res* **621**, 59–64.

Yi HA, Yi SD, Jang BC, Song DK, Shin DH, Mun KC, Kim SP, Suh SI & Bae JH (2005). Inhibitory effects of glucosamine on lipopolysaccharide-induced activation in microglial cells. *Clin Exp Pharmacol Physiol* **32**, 1097–1103.

Zhang L, McLarnon JG, Goghari V, Lee YB, Kim SU & Krieger C (1998). Cholinergic agonists increase intracellular Ca^{2+} in cultured human microglia. *Neurosci Lett* **255**, 33–36.

Acknowledgements

We thank Carolyn E. Oki-Idouchi, Ka'ohimanu Dang and Mahealani K. Monteilh-Zoller for excellent technical support. This work was supported by NIH grant R01 NS40927 (R.P.) and Deutsche Forschungsgemeinschaft fellowship BE-2616/1-1 (A.B.).